

Z + Jets Cross Section Ratio Measurements

Marc Buehler

P.O. Box 500, Fermilab, MS 352, Batavia, IL 60657

Abstract. We present a study of events with Z bosons and jets produced at the Fermilab Tevatron Collider in $p\bar{p}$ collisions at a center of mass energy of 1.96 TeV. The data sample consists of nearly 14,000 $Z/\gamma^* \rightarrow e^+e^-$ candidates corresponding to the integrated luminosity of 340 pb^{-1} collected using the DØ detector. Ratios of the $Z/\gamma^* + \geq n$ jet cross sections to the total inclusive Z/γ^* cross section have been measured for $n = 1$ to 4 jet events. Our measurements are found to be in good agreement with a next-to-leading order QCD calculation and with a tree-level QCD prediction with parton shower simulation and hadronization.

Keywords: Jets, QCD, Z Bosons

PACS: 13.38.Dg, 14.70.Hp, 13.87.-a, 12.38.Aw, 12.38.Qk, 13.85.-t

INTRODUCTION

Leptonic decays of the electroweak gauge bosons, W^\pm and Z , produced in association with jets are prominent signatures at present and future hadron colliders. Measurements of $W/Z + \geq n$ jet cross sections are important for understanding perturbative quantum chromodynamics (QCD) calculations and for developing Monte Carlo (MC) simulation programs capable of handling partons in the final state at leading order (LO), or in some cases, next-to-leading order (NLO). Furthermore, the associated production of W/Z bosons with jets represents a significant background to Higgs boson searches, as well as other standard model processes of interest such as top quark production, and many new physics searches at the Fermilab Tevatron Collider and the CERN Large Hadron Collider.

Measurements of $Z + \geq n$ jet cross sections with lower integrated luminosity and center of mass energy have been performed previously by the CDF collaboration [1]. In this study, we present the first measurement of the ratios of the $Z/\gamma^* + \geq n$ jet production cross sections to the total inclusive Z/γ^* cross section for jet multiplicities $n = 1 - 4$ in $p\bar{p}$ collisions at $\sqrt{s} = 1.96$ TeV. These results are based on a data sample corresponding to an integrated luminosity of 340 pb^{-1} accumulated with the DØ detector.

THE DØ DETECTOR

The elements of the DØ detector [2] of primary importance to this analysis are the uranium/liquid-argon sampling calorimeter and the tracking system. The DØ calorimeter has a granularity of $\Delta\eta \times \Delta\phi = 0.1 \times 0.1$ forming projective towers, where η is the pseudorapidity ($\eta = -\ln[\tan(\theta/2)]$), θ is the polar angle with respect to the proton beam), and ϕ is the azimuthal angle. The calorimeter has a central section covering pseudorapidities up to ≈ 1.1 , and two end calorimeters that extend the coverage to

$|\eta| \approx 4.2$. The tracking system consists of a silicon micro-strip tracker and a central fiber tracker, both located within a 2 T superconducting solenoidal magnet, with designs optimized for tracking and vertexing at pseudorapidities of $|\eta| < 3$ and $|\eta| < 2.5$, respectively.

EVENT SELECTION

The data sample for this analysis [3] was collected between April 2002 and June 2004. Events from $Z/\gamma^* \rightarrow e^+e^-$ decays were selected with a combination of single-electron triggers, based on energy deposited in calorimeter towers ($\Delta\eta \times \Delta\phi = 0.2 \times 0.2$). Final event selection was based on detector performance, event properties, and electron and jet identification criteria.

Events were required to have a reconstructed primary vertex with a longitudinal position within 60 cm of the detector center. Electrons were reconstructed from electromagnetic (EM) clusters in the calorimeter using a simple cone algorithm. The two highest- p_T electron candidates in the event, both having transverse momenta $p_T > 25$ GeV, were used to reconstruct the Z boson candidate. Both electrons were required to be in the central region of the calorimeter $|\eta_{\text{det}}| < 1.1$ (pseudorapidity η_{det} is calculated with respect to the center of the detector) with at least one of the electrons having fired the trigger(s) for the event. The electron pair was required to have an invariant mass consistent with the Z boson mass, $75 \text{ GeV} < M_{ee} < 105 \text{ GeV}$.

To reduce background contamination, mainly from jets misidentified as electrons, the EM clusters were required to pass three quality criteria based on the shower profile: (i) the electron had to deposit at least 90% of its energy in the 21-radiation-length EM calorimeter (ii) the lateral and longitudinal shape of the energy cluster had to be consistent with those of an electron, and (iii) the electron had to be isolated from other energy deposits in the calorimeter with isolation fraction $f_{\text{iso}} < 0.15$. The isolation fraction is defined as $f_{\text{iso}} = [E(0.4) - E_{\text{EM}}(0.2)]/E_{\text{EM}}(0.2)$, where $E(R_{\text{cone}})$ ($E_{\text{EM}}(R_{\text{cone}})$) is the total (EM) energy within a cone of radius $R_{\text{cone}} = \sqrt{(\Delta\eta)^2 + (\Delta\phi)^2}$ centered around the electron. Additionally, at least one of the electrons was required to have a spatially matched track associated with the reconstructed calorimeter cluster, and the track momentum had to be consistent with the energy of the EM cluster. A total of 13,893 events passed the selection criteria.

Jets were reconstructed using the ‘‘Run II cone algorithm’’ [4] which combines particles within a cone of radius $R_{\text{cone}} = 0.5$. Spurious jets from isolated noisy calorimeter cells were eliminated by cuts on the jet energy deposition pattern. Jets were required to be confirmed by energy deposits as measured by the trigger readout. The transverse momentum of each jet was corrected for multiple $p\bar{p}$ interactions, calorimeter noise, out-of-cone showering effects, and energy response of the calorimeter as determined from the missing transverse energy balance of photon-jet events. Jets were required to have $p_T > 20$ GeV and $|\eta| < 2.5$; jets were eliminated if they overlapped with the electrons coming from the Z boson decay within $\Delta R = \sqrt{(\Delta\eta)^2 + (\Delta\phi)^2} = 0.4$. Small jet losses due to this separation cut from the Z boson electrons were estimated as a function of the number of associated jets using a PYTHIA [5] event generator MC sample.

EFFICIENCIES

The electron efficiencies for trigger, track matching, reconstruction, and identification were determined from data, based on a “tag-and-probe” method. Z candidates were selected with one electron (tag) satisfying a tighter track-matching requirement to further reduce background contamination, and another electron (probe) with all other cuts applied except the one under study. The fraction of events with probe electrons passing the requirement under study determined the efficiency of a given cut. The overall trigger efficiency for Z candidates that survived the analysis selection cuts was found to be greater than 99%. The electron reconstruction and identification efficiencies were measured as a function of azimuthal angle and p_T , and the average efficiency was found to be about 89%. The spatial and energy combined track-matching efficiency was measured to be about 77%. The electron reconstruction, selection, trigger, and track-matching efficiencies were examined as a function of jet multiplicity. No significant variations of the efficiencies were observed, except for the track-matching efficiency for which the multiplicity dependence was taken into account to correct the data.

The kinematic and detector geometric acceptance for electrons from Z/γ^* decays in the mass region of $75 \text{ GeV} < M_{ee} < 105 \text{ GeV}$ and with the primary vertex within 60 cm of the detector center was determined as a function of jet multiplicity. For the acceptance calculation of the inclusive Z/γ^* sample, an inclusive PYTHIA sample was used. The inclusive PYTHIA events were weighted so that the p_T distribution of the Z boson in the MC agreed with data. For the jet-multiplicity dependence of the acceptance calculation, a $Z/\gamma^* + n$ parton leading-order generator was used [6], with the evolution of partons into hadrons carried out by PYTHIA. All the samples were processed through the full DØ detector simulation based on GEANT [7] and the DØ reconstruction software. The overall dielectron acceptance for the $Z/\gamma^* + \geq 4$ jet sample was found to be about 30% higher than the acceptance for the Z/γ^* inclusive sample.

The reconstruction and identification efficiency of jets was determined from a MC sample with full detector simulation processed with the same analysis procedure as the data. A scaling factor was applied to the MC jets to adjust their reconstruction and identification efficiency to that of data jets using the “ Z p_T -balance” method. In events selected with Z candidates, a search for a recoiling jet opposite to the Z boson in azimuthal angle was performed. The probability of finding a recoiling jet as a function of the Z p_T was measured in data and MC. The ratio of these probabilities defined the scaling factor that was applied to the MC jets. After applying the scaling factor, the jet reconstruction and identification efficiency was determined by matching particle-level jets (i.e., jets found from final state particles after parton hadronization) to calorimeter jets. The efficiency was parameterized as a function of particle-level jet p_T , where the p_T values were smeared with the data jet energy resolutions, measured in three η regions of the calorimeter. As a cross check, the scaling factor determined from the “ Z p_T -balance” method was compared to a scaling factor using a photon+jet sample. The two scaling factors were found to be consistent.

TABLE 1. Cross-section ratios with statistical and systematic uncertainties (all $\times 10^{-3}$) for different inclusive jet multiplicities.

Multiplicity ($Z/\gamma^* + \geq n$ jets)	≥ 1	≥ 2	≥ 3	≥ 4
R_n	120.1	18.6	2.8	0.90
Total Statistical Uncertainty	± 3.3	± 1.4	± 0.56	± 0.44
Total Systematic Uncertainty	$-17.1, +15.6$	$-5.0, +6.2$	$-1.06, +1.43$	$-0.40, +0.48$
Jet Energy Calibration	± 11.7	± 3.3	± 0.74	± 0.23
Jet Reconstruction/Identification	$-7.0, +2.2$	$-2.9, +4.3$	$-0.64, +0.82$	$-0.30, +0.40$
Unsmearing Procedure	$-3.6, +2.2$	$-1.6, +2.4$	$-0.24, +0.85$	$-0.08, +0.09$
Jet Energy Resolution	$-2.7, +3.4$	$-0.04, +0.13$	$-0.17, +0.15$	$-0.03, +0.04$
Acceptance	± 1.8	± 0.7	± 0.10	± 0.003
Efficiencies (Trigger, EM, Track)	± 8.5	± 1.3	± 0.20	± 0.07
Electron-Jet-Overlap	± 3.2	± 0.7	± 0.14	± 0.05

BACKGROUNDS

The primary source of background to the Z/γ^* dielectron signal is from multijet production from QCD processes in which the jets have a large electromagnetic component or they are mismeasured in some way that causes them to pass the electron selection criteria. For the $Z/\gamma^* + \geq 0 - 2$ jet samples, a convoluted Gaussian/Breit-Wigner function was used to fit the Z resonance, and an exponential shape was used to account for both the QCD background and the Drell-Yan component of the signal. In the case of the lower statistics $Z/\gamma^* + \geq 3$ jet sample, the contributions due to the QCD and Drell-Yan components were estimated based on the side bands of the dielectron invariant mass spectrum. In each case, a PYTHIA sample was used to disentangle the QCD component from the Drell-Yan contribution. The background contribution for the $Z/\gamma^* + \geq 4$ jet multiplicity sample was estimated by extrapolating an exponential fit to the QCD background of the $0 - 3$ jet multiplicity bins. There are also contributions to the Z/γ^* candidates that are not from misidentification of electrons, but correspond to standard model processes (e.g., $t\bar{t}$ production, $Z \rightarrow \tau^+\tau^-$, $W \rightarrow e\nu$). Such irreducible background contributions were taken into account, but found to be small.

UNSMEARING

The cross sections as a function of jet multiplicity were corrected for jet reconstruction and identification efficiencies, and for event migration due to the finite jet energy resolution of the detector. The correction factors were determined using two independent event generator samples, both tuned to match the measured inclusive jet multiplicity and jet p_T distributions in data. The first sample was based on PYTHIA simulations. The second sample (ME-PS) was based on MADGRAPH [8] $Z/\gamma^* + n$ LO Matrix Element (ME) predictions using PYTHIA for parton showering (PS) and hadronization, and a modified CKKW [9] method to map the $Z/\gamma^* + n$ parton event into a parton shower history [10]. The ME-PS predictions were produced with MADGRAPH tree level processes of up to three partons. Both of these samples contained only particle-level jets (i.e., no detector simulation). The p_T of the jets was smeared with the data jet energy resolutions. Sub-

sequently, jets were removed from the sample according to the measured jet reconstruction/identification efficiencies. The ratio between the two inclusive jet multiplicity distributions (the generated distribution and the one with the jet reconstruction/identification efficiency and energy resolution applied) determined the unsmearing correction factors for a given MC sample. The weighted averages of the correction factors corresponding to the two MC samples as a function of jet multiplicity were applied to correct the data jet multiplicity spectrum. The differences between the correction factors from the two MC samples contribute to the systematic uncertainty of the procedure. Another source of systematic uncertainty was determined from a closure test estimated by applying the full unsmearing procedure to a MC control sample. The unsmearing correction factors range from 1.11 to 2.9 for the $Z/\gamma^* + \geq 1$ to $Z/\gamma^* + \geq 4$ jet multiplicity samples respectively.

CROSS SECTION RATIOS

The fully corrected ratios, R_n , of the $Z/\gamma^* + \geq n$ jet production cross sections to the inclusive Z/γ^* cross section

$$R_n \equiv \frac{\sigma(Z/\gamma^* + \geq n \text{ jets})}{\sigma(Z/\gamma^*)} \quad (1)$$

for the mass region $75 \text{ GeV} < M_{ee} < 105 \text{ GeV}$ are summarized in Table 1. Systematic uncertainties include contributions from the jet energy calibration corrections, jet reconstruction and identification efficiency, unsmearing procedure, jet energy resolution, and variations in the acceptance coming from samples with different event generators. They also take into account uncertainties in the variation of efficiencies for trigger, electron reconstruction, identification, and track matching as a function of jet multiplicity, as well as uncertainties due to the electron-jet overlap correction. All these uncertainties are assumed to be uncorrelated and they are added in quadrature to estimate the total systematic uncertainty. The statistical uncertainties include contributions from the number of candidate events, background estimation, acceptance, efficiencies, and unsmearing correction.

Figure 1 shows the fully corrected measured cross-section ratios for $Z/\gamma^* + \geq n$ jets as a function of jet multiplicity, compared to three QCD predictions. MCFM [11] is a NLO calculation for up to $Z/\gamma^* + 2$ parton processes. The CTEQ6M [12] parton distribution function (PDF) set was used, and the factorization and renormalization scales $\mu_{F/R}$ were set to the Z boson mass, M_Z . The ME-PS predictions have been normalized to the measured $Z/\gamma^* + \geq 1$ jet cross-section ratio. The CTEQ6L PDF set was used, and the factorization scale was set to $\mu_F = M_Z$. The renormalization scale was set to $\mu_R = p_{T \text{ jet}}$ for jets from initial state radiation and $\mu_R = k_{T \text{ jet}}$ for jets from final state radiation ($k_{T \text{ jet}}$ is the transverse momentum of a radiative jet relative to its parent parton momentum direction). The PYTHIA predictions have been normalized to the measured $Z/\gamma^* + \geq 1$ jet cross-section ratio. The CTEQ5L [13] PDF set was used, and the factorization and renormalization scales were set to $\mu_{F/R} = M_Z$. The MCFM and ME-PS predictions are generally in good agreement with the data. PYTHIA predicts fewer events with high jet multiplicity due to missing higher order contributions at the hard-scatter level.

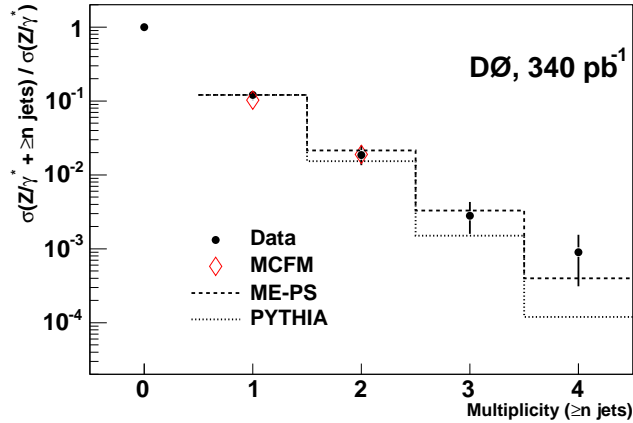


FIGURE 1. Ratios of the $Z/\gamma^* + \geq n$ jet cross sections to the total inclusive Z/γ^* cross section versus jet multiplicity. The uncertainties on the data points (dark circles) include the combined statistical and systematic uncertainties added in quadrature. The dashed line represents the predictions of LO Matrix Element (ME) calculations using PYTHIA for parton showering (PS) and hadronization, normalized to the measured $Z/\gamma^* + \geq 1$ jet cross-section ratio. The dotted line represents the predictions of PYTHIA normalized to the measured $Z/\gamma^* + \geq 1$ jet cross-section ratio. The open diamonds represent the MCFM predictions.

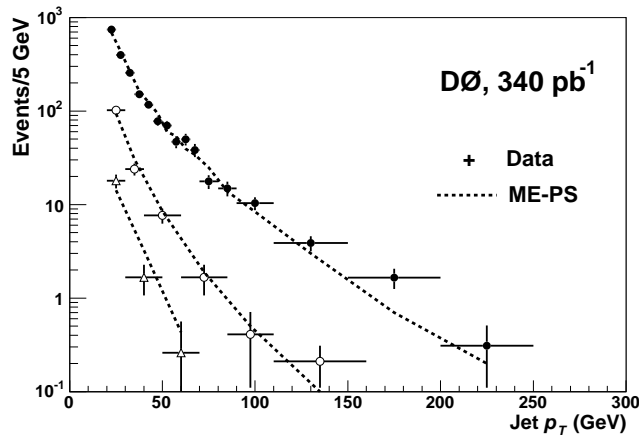


FIGURE 2. Comparison between data and theory (ME-PS) for the highest p_T jet distribution in the $Z/\gamma^* + \geq 1$ jet sample (dark circles) for the second highest p_T jet distribution in the $Z/\gamma^* + \geq 2$ jet sample (open circles) and for the third highest p_T jet distribution in the $Z/\gamma^* + \geq 3$ jet sample (open triangles). The uncertainties on the data are only statistical. The MC distributions are normalized to the data.

Figure 2 compares jet p_T spectra of the n^{th} jet, $n = 1, 2, 3$, in $Z/\gamma^* + \geq n$ jet events to ME-PS MC predictions. The MC events have been passed through the full detector simulation. The MC jet p_T spectra have been normalized separately to the data distributions. Good agreement can be seen over a wide range of jet transverse momenta.

CONCLUSIONS

In summary, we have presented the first measurements of the ratios of the $Z/\gamma^* + \geq n$ jet ($n = 1 - 4$) production cross sections to the total inclusive Z/γ^* cross section from $p\bar{p}$ collisions at $\sqrt{s} = 1.96$ TeV. The measured ratios of cross sections were found to be in good agreement with MCFM and an enhanced leading-order matrix element prediction with PYTHIA-simulated parton showering and hadronization. PYTHIA simulations alone exhibit a deficit of high jet multiplicity events.

ACKNOWLEDGMENTS

We thank S. Mrenna for providing the ME-PS event simulation sample.

REFERENCES

1. F. Abe *et al.* (CDF Collaboration), Phys. Rev. Lett. **77**, 448 (1996).
2. V. Abazov *et al.* (DØ Collaboration), Fermilab-Pub-05-341-E.
3. M. Buehler, Ph.D. Dissertation, University of Illinois at Chicago, Fermilab-Thesis-2005-42 (2005).
4. G.C. Blazey *et al.*, in Proceedings of the Workshop: "QCD and Weak Boson Physics in Run II," edited by U. Baur, R.K. Ellis, and D. Zeppenfeld, p. 47, Fermilab-Pub-00/297 (2000).
5. T. Sjöstrand, Computer Physics Commun. **135**, 238 (2001).
6. M.L. Mangano, M. Moretti, F. Piccinini, R. Pittau, and A. Polosa, J. High Energy Phys. **07**, 001 (2003).
7. R. Brun and F. Carminati, CERN Program Library Long Writeup W5013, 1993 (unpublished).
8. F. Maltoni and T. Stelzer, J. High Energy Phys. **0302**, 027 (2003).
9. S. Catani, F. Krauss, R. Kuhn and B. R. Webber, J. High Energy Phys. **0111**, 063 (2001) [arXiv:hep-ph/0109231].
F. Krauss, J. High Energy Phys. **0208**, 015 (2002) [arXiv:hep-ph/0205283].
10. S. Mrenna and P. Richardson, J. High Energy Phys. **0405**, 040 (2004) [arXiv:hep-ph/0312274].
11. J. Campbell and R.K. Ellis, Phys. Rev. D **65**, 113007 (2002).
12. J. Pumplin *et al.*, J. High Energy Phys. **0207**, 12 (2002).
13. H.L. Lai *et al.*, Eur. Phys. J. **C12**, 375 (2000).